CTU Journal of Innovation and Sustainable Development
ISSN 2588-1418 | e-ISSN 2815-6412

DOI:10.22144/ctujoisd.2024.301

Removal of tetracycline antibiotic from aqueous solution using bimetallic CuCo-ZIFs as an efficient catalyst in the presence of hydrogen peroxide

Le Thi Anh Thu[1], Tran Bao Bao[1], Ho Ngoc Tri Tan[1], Cao Luu Ngoc Hanh[1], Ngo Truong Ngoc Mai[1], Luong Huynh Vu Thanh[1,2], and Dang Huynh Giao[1,2*]

[1]*College of Engineering, Can Tho University, Viet Nam*

[2]*Applied Chemical Engineering Lab, College of Engineering, Can Tho University, Viet Nam*

**Corresponding author (dhgiao@ctu.edu.vn)*

Article info.

Received 31 Jan 2024
Revised 25 Feb 2024
Accepted 26 Feb 2024

Keywords

Advanced oxidation process, bimetallic ZIF-67, hydrogen peroxide, tetracycline removal, zeolitic-imidazole frameworks

ABSTRACT

Antibiotics play an important role in disease treatment; however, they are also a threat to public health and the ecosystem. Therefore, a bimetallic CuCo-ZIFs catalyst was manufactured through the ultrasonic-assisted solvothermal method to activate H_2O_2 towards the removal of tetracycline (TC) in an aqueous environment, a polluting broad-spectrum antibiotic model. PXRD, SEM, TEM, EDX, TGA, FT-IR, and BET analyses indicated that CuCo-ZIFs cubic crystals were successfully synthesized with high crystallinity, large specific surface area, and ideal thermal stability. Factors affecting the TC removal were investigated, including CuCo-ZIFs dosage, H_2O_2 concentration, treatment time, initial TC concentration, and reaction temperature. The results showed that the CuCo-ZIFs/H_2O_2 catalytic system was capable of effectively handling TC, with about 93.9% of TC removed in the presence of 0.3 g.L^{-1} CuCo-ZIFs, 0.01 mol.L^{-1} H_2O_2 at room temperature within 30 min. Conclusively, this study contributes to expanding the application potential of bimetallic CuCo-ZIFs materials to eliminate antibiotic residues in an aqueous environment and inspire research on environmental improvement.

1. INTRODUCTION

Environmental pollution, especially water pollution, induced by the presence of persistent organic compounds, including dyes, pesticides, and antibiotics residue, has become an urgent global concern. Therein, tetracycline (TC) belongs to the group of broad-spectrum antibiotics widely used for aquaculture, veterinary purposes, within the pharmaceutical industry, and human disease treatment (Wang et al., 2022). Therefore, TC is frequently present in the aquatic environment via organism excretion (Xu et al., 2021). The accumulation of tetracyclines (TC) in the environment over time can promote the proliferation of antibiotic-resistant bacteria, posing a significant threat to ecosystem integrity and public health (Ben et al., 2019). For these reasons, the removal of TC residues from wastewater is a pressing issue that needs to be addressed.

A variety of different methods have been applied to address this problem, including adsorption (Liu et al., 2021), coagulation (Lu et al., 2021), flocculation (Yang et al., 2015), and membrane filtration techniques (Liu et al., 2017). However, TC removal efficiency of the above approaches is mainly based on collecting, concentrating TC molecules, or only transferring them into a different phase, without actually decomposing TC (Fan et al., 2021). Accordingly, advanced oxidation processes (AOPs) have been recognized as a potential method to

overcome these shortcomings due to their ability to mineralize and degrade organic pollutants in water based on the generation of highly active oxidizing radicals such as hydroxyl ($^{\bullet}OH$) and sulfate ($SO_4^{\bullet-}$) (Honarmandrad et al., 2023). The oxidants in the AOPs are usually activated by irradiation (Lei et al., 2021), ultrasonication (Ince, 2018), electrochemical reaction (Lima et al., 2020), catalysis (Zhang et al., 2022a) or a combination of the above methods (Takdastan et al., 2018). For example, classic Fenton process is an effective AOPs based on the promotion of $^{\bullet}OH$ radical generated by Fe^{2+}/H_2O_2 system. Unfortunately, the process operates in a narrow pH range with non-reusable catalysts and may cause secondary pollution related to iron sludge produced after the reaction (Wang et al., 2021b). Hence, the development of catalysts with outstanding stability, effective oxidant activation, and easy recovery is a challenge to solve.

In recent decades, zeolitic imidazolate frameworks (ZIFs), which are a common sub-family of metal organic frameworks (MOFs), have shown potential for persistent organic matter removal in water due to many outstanding properties. ZIFs consist of transition metal ions (such as Zn^{2+}, Co^{2+}) coordinating with the 2-methylimidazole ligand (Wang et al., 2021a). Inheriting the unique structure combining inorganic and organic components from MOFs, ZIFs possess a diverse porous crystalline structure, large specific surface area, open catalytic active sites and tunable pores, and high thermal and chemical stability (Ighalo et al., 2022). Among them, ZIF-67, composed of cobalt ions and 2-methylimidazole (2-MIm) bridges, has attracted increasing interest because they have most of the above characteristics and can be synthesized at room temperature and atmospheric pressure (Park et al., 2006). Based on the aforementioned features, ZIF-67 promises to effectively activate oxidants in AOPs. Impressively, bimetallic ZIFs with the addition of metal ions to ZIF-67 are reported to have improved properties and catalytic performance compared to pristine materials (Yao et al., 2021). In particular, Abuzalat et al. (2022) reported that the bimetallic Co-Zn-ZIF-8 catalyst effectively activated H_2O_2 to degrade methyl orange dye with an initial concentration of 10 $mg.L^{-1}$, achieving 90% efficiency in about 50 min. In another study, Zhang et al. (2022b) successfully synthesized copper and cobalt nanoparticle decorated carbon frameworks (Cu/Co@CF) and demonstrated that material extended the pore volume and carried more active centers than monometallic ZIF-67 with removal efficiency of 4-nitrophenol reaching 99.7% within only 1 min.

Herein, bimetallic CuCo-ZIFs were prepared by facile ultrasonic-assisted solvothermal method. The obtained material has a porous crystalline structure, large specific surface area and high thermal stability. Under the influence of various metal centers including Cu^{2+} and Co^{2+} contained in CuCo-ZIFs and the presence of H_2O_2, hydroxyl radicals are produced and effectively removed for TC antibiotics. Factors affecting the reaction process were also investigated, including catalyst dosage, H_2O_2 concentration, treatment time, reaction temperature and initial TC concentration. This study contributes to expanding the application of CuCo-ZIFs for removing antibiotic residues from water using AOPs.

2. MATERIALS AND METHOD

2.1. Chemicals and materials

The chemicals used in this study included 2-MIm ($C_4H_6N_2$, 99%, Acros), copper (II) nitrate trihydrate ($Cu(NO_3)_2.3H_2O$, 99%, China), cobalt nitrate hexahydrate ($Co(NO_3)_2.6H_2O$, 99%, China), ethanol (EtOH, C_2H_5OH, 99.7%, China), hydrogen peroxide (H_2O_2, 30 wt%, China), and tetracycline hydrochloride ($C_{22}H_{24}N_2O_8.HCl$, China).

2.2. Preparation of CuCo-ZIFs

CuCo-ZIFs were synthesized by an ultrasonic-assisted solvothermal method. The synthesis process was conducted according to a reported method with slight modifications (Dang et al., 2021). Herein, the molar ratio of metal salts:2-MIm and Cu^{2+}:Co^{2+} was fixed to 1:4 and 1:1, respectively. Typically, the ethanolic solutions of 2-MIm (0.6568 g/ 20 mL), $Cu(NO_3)_2.3H_2O$ (0.2416 g/ 10 mL), and $Co(NO_3)_2.6H_2O$ (0.291 g/ 10 mL) were separately prepared. Next, Cu^{2+} solution was added to Co^{2+} solution and stirred for 10 min. Subsequently, the homogeneous salt mixture was added drop by drop into 2-MIm solution to form a purple suspension. The obtained suspension was ultrasonicated for 15 min. Then, the mixture was aged for 24 hours to facilitate crystal formation. The precipitate was collected by centrifugation at 4000 rpm for 15 min, washed repeatedly with EtOH and finally dried overnight at 60°C. The purple crystals obtained after drying were the CuCo-ZIFs. Besides, ZIF-67 (Co-ZIFs) was also prepared following the same method with $Co(NO_3)_2.6H_2O$ (0.5821 g, 2 mmol), and 2-MIm (0.6568 g, 8 mmol) in 40 mL EtOH, and no copper salt (Giao et al., 2019).

Furthermore, some other heterogeneous catalysts were also synthesised using the previous procedure with slight modifications, including FeCo-ZIFs, FeZn-ZIFs, NiZn-ZIFs, Co-ZIFs, and Zn-ZIFs. Typically, FeCo-ZIFs were synthesised by 24 mmol of 2-MIm, 0.25 mmol of $FeSO_4.7H_2O$, and 1.25 mmol of $Co(NO_3)_2.6H_2O$ in 20 mL MeOH (Hu et al., 2018). Similarly, FeZn-ZIFs were prepared by 40 mmol of 2-MIm, 9 mmol of $Zn(NO_3)_2.6H_2O$, and 1 mmol of $FeSO_4.7H_2O$ in 60 mL MeOH (Le et al., 2023). NiZn-ZIFs were obtained by 20 mmol of 2-MIm, 1 mmol of $Ni(NO_3)_2.6H_2O$, and 4 mmol of $Zn(NO_3)_2.6H_2O$ in 40 mL MeOH (Yao et al., 2020). Zn-ZIFs (ZIF-8) were generated by 4 mmol of 2-MIm, and 1 mmol of $Zn(NO_3)_2.6H_2O$ in 20 mL MeOH (Wang et al., 2020).

2.3. Characterizations of catalyst

Structure and morphological characterizations of CuCo-ZIFs, Co-ZIFs, and other relevant substances/ materials were examined by powder X-ray diffraction using Cu K_α radiation (PXRD, Empyrean-PANanlytical powder diffractometer). Diffraction peaks were recorded in the range from 5 to 50 degrees for 2θ. Fourier-transform infrared spectroscopy was measured from 4000 to 400 cm^{-1} to analyse the molecular structure and functional group of CuCo-ZIFs (FT-IR, PerkinElmer MIR/NIR Frontier instrument). Thermogravimetric analysis was conducted with a heating rate of 10°C.min^{-1} from room temperature to 900°C (TGA, LabSys Evo equipment). The surface topography and structure of CuCo-ZIFs were obtained by scanning electron microscopy (SEM, Hitachi S-4800), and transmission electron microscopy (TEM, JEM-1400) with an Emax energy for Energy dispersive X-ray spectroscopy (EDX) analysis to detect the chemical elements. The specific surface areas of the CuCo-ZIFs were measured on Brunauer–Emmett–Teller model (BET). UV-Vis spectrophotometer (Labomed, UVD-3500) was used to determine the concentration of TC.

2.4. Catalytic experiments of CuCo-ZIFs

In the TC removal process, H_2O_2 was employed as an oxidizing agent, while CuCo-ZIFs served as a heterogeneous catalyst to activate H_2O_2, generating free hydroxyl radicals. The TC removal system was performed sequentially by changing the levels of the investigation factors and fixing the remaining factors. The factors affecting TC removal efficiency which were investigated including CuCo-ZIFs dosage (0-0.5 $g.L^{-1}$), H_2O_2 concentration (0.1-0.5 $mol.L^{-1}$), reaction time (10-50 min), reaction temperature (room temperature to 60ºC), and initial TC concentration (10-60 $mg.L^{-1}$). Except for the experiment investigating CuCo-ZIFs dosage, the experiments were conducted by dispersing 3 mg CuCo-ZIFs into 10 mL of 30 $mg.L^{-1}$ TC solution, in the presence of 0.1 $mol.L^{-1}$ H_2O_2 at room temperature. After 30 min, the solution was collected by filtration and UV-Vis spectroscopic measured at the maximum absorption wavelength of 357 nm. TC removal efficiency by CuCo-ZIFs/H_2O_2 system was determined by the equation (1). All experiments were conducted in triplicate, and the results were reported as the mean ± standard deviation (SD).

$$\text{Removal efficiency (\%)} = \left(1 - \frac{C_e}{C_0}\right) \times 100 \quad (1)$$

Whereas C_0, C_e represented the concentrations of the initial TC ($mg.L^{-1}$) and the residual TC ($mg.L^{-1}$), respectively.

3. RESULTS AND DISCUSSION

3.1. Characterization of CuCo-ZIFs

The results of the structural characteristic analysis of CuCo-ZIFs catalyst presented in Figure 1 are consistent with the previous research (Dang et al., 2021). The PXRD results showed that CuCo-ZIFs had characteristic crystalline peaks almost identical to Co-ZIFs and previously reported CuCo-ZIFs, demonstrating that the catalyst was successfully synthesized (Figure 1a). Significantly, three diffraction peaks in the PXRD pattern of CuCo-ZIFs were at positions 7.3º, 10.4º and 12.7º, corresponding to the crystal faces of (011), (002) and (112), respectively, indicating the obtained catalyst had high crystallinity.

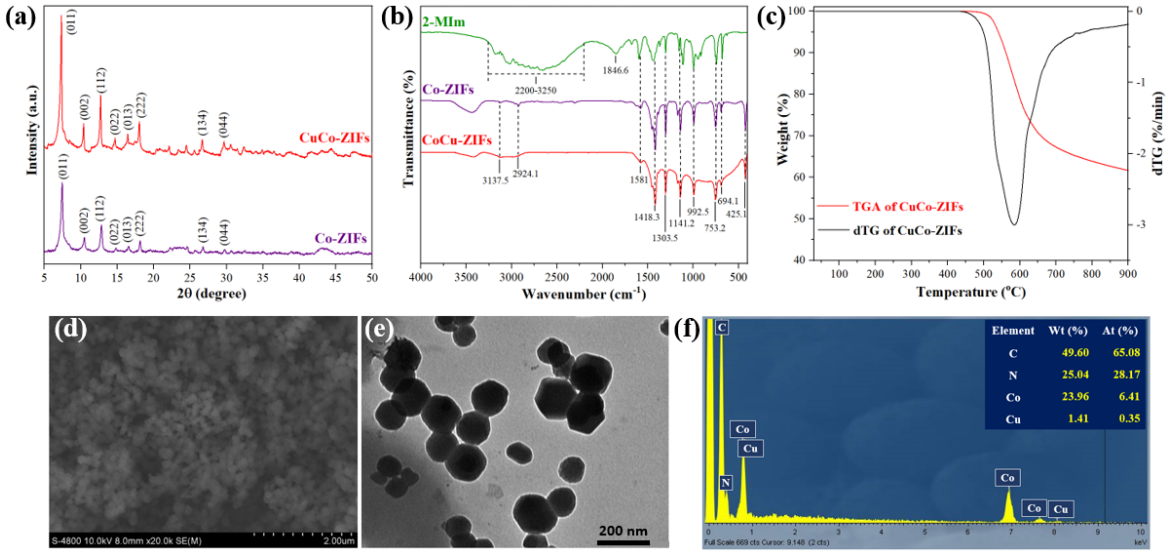

Figure 1. PXRD pattern of CuCo-ZIFs, Co-ZIFs (a), FT-IR spectrum of CuCo-ZIFs, Co-ZIFs, 2-MIm (b), TGA curve of CuCo-ZIFs (c), SEM image of CuCo-ZIFs (d), TEM image of CuCo-ZIFs (e), and EDX spectra of CuCo-ZIFs (f)

The FT-IR spectrum of CuCo-ZIFs was compared with that of Co-ZIFs and 2-MIm to confirm the functional groups on the material surfaces (Figure 1b). For all three spectra, the peak at 1581 cm^{-1} was assigned to the C=N stretching vibration of the imidazole ring, while the range between 2200 and 3250 cm^{-1} corresponded to the N–H hydrogen bonding interactions among the 2-MIm ligands (Ulu, 2020). The 2-MIm characteristic band at 1846.6 cm^{-1} (N–H stretching vibration) completely vanished in Co-ZIFs and CuCo-ZIFs, which could be due to the deprotonation to form a new bond between the metal and N. Accordingly, the band at 425.1 cm^{-1} appeared in the spectrum of Co-ZIFs and CuCo-ZIFs, which was assigned to the metal-N stretching vibration, did not presented in 2-MIm, indicating that the ion metal was successfully linked together through 2-MIm bridges at the N site.

In addition, TGA curve of CuCo-ZIFs showed that the material had high thermal stability of above 550°C (Figure 1c). Moreover, the surface areas of CuCo-ZIFs were determined as up to 1797.5 $m^2.g^{-1}$ using the BET model with the pore size of 14.6 Å. The SEM (Figure 1d) and TEM (Figure 1e) images showed that the particles of CuCo-ZIFs exhibited a uniform cubic shape with an average size of about 150 nm. The clear and smooth crystal surface indicated that the participation of copper did not affect the morphology of the Co-ZIFs framework. Finally, the presence of elemental components of C, N, Co, and especially Cu, as shown in the EDX spectra (Figure 1f), once again demonstrated the successful combination of Cu and Co-ZIFs to form CuCo-ZIFs.

3.2. TC removal efficiency of CuCo-ZIFs/H_2O_2 system

Firstly, the role of CuCo-ZIFs in the TC removal process was demonstrated by investigating the CuCo-ZIFs dosages in the range of 0 to 0.5 $g.L^{-1}$ while keeping the remaining factors including H_2O_2 concentration of 0.015 $mol.L^{-1}$, the initial TC concentration of 30 $mg.L^{-1}$, reaction time of 30 min, and room temperature (Figure 2). Apparently, only about 11.4% of TC was removed by H_2O_2, which was significantly lower than that when adding the CuCo-ZIFs catalyst, implying that CuCo-ZIFs plays a key role in this study. Accordingly, the increase in the dosage of CuCo-ZIFs from 0.1 to 0.3 $g.L^{-1}$ increased TC removal efficiency from 78.4% to 93%, respectively, which may be due to the addition of the catalytic metal center that promotes active-species production. However, when continuing to increase the catalyst dosage of CuCo-ZIFs to 0.4 $g.L^{-1}$ and 0.5 $g.L^{-1}$, the efficiency slightly decreased to 92.6% and 92.3%, respectively. This may be due to the non-selectivity of the produced hydroxyl radicals (Nidheesh & Rajan, 2016). Therefore, the next experiments were conducted under the condition of the CuCo-ZIFs dosage at 0.3 $g.L^{-1}$.

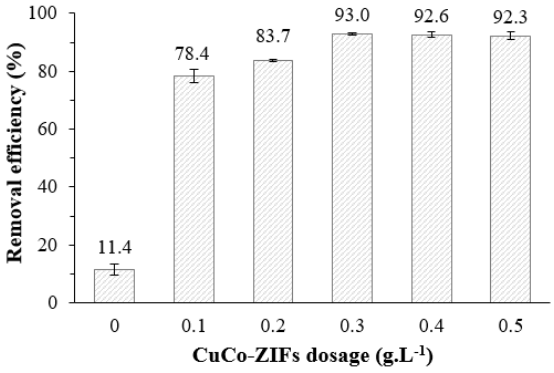

Figure 2. The removal efficiency of TC in various CuCo-ZIFs dosages

Implementation conditions: H_2O_2 concentration = 0.015 mol.L^{-1}, time = 30 min, room temperature, initial TC concentration = 30 mg.L^{-1}.

Secondly, as H_2O_2 acts as an oxidant to provide active species under the activation of CuCo-ZIFs catalyst, the effect of H_2O_2 concentrations (0.1-0.5 mol.L^{-1}) on TC removal efficiency was carried out at room temperature, CuCo-ZIFs dosage of 0.3 g.L^{-1}, the initial TC concentration of 30 mg.L^{-1} within 30 min (Figure 3a). The CuCo-ZIFs/H_2O_2 system had a relatively high TC removal efficiency. In particular, only a small amount of H_2O_2 concentration of 0.005 mol.L^{-1} could remove 92.1% of TC, which increased to 93.9% at an H_2O_2 concentration of 0.01 mol.L^{-1}. However, the TC removal efficiency tended to decrease to 93%, 92.5%, and 90.3% when using H_2O_2 at concentrations of 0.015, 0.020 and 0.025 mol.L^{-1}, respectively. The excess H_2O_2 would scavenge the active low-selectivity •OH radicals, which can attack each other or even H_2O_2 and reduce the overall efficiency of the whole process (Nidheesh & Rajan, 2016). Accordingly, the H_2O_2 concentration of 0.01 mol.L^{-1} was the appropriate level to conduct further experiments.

Thirdly, the TC removal time was considered with a series of experiments ranging from 10 to 50 minutes at room temperature, CuCo-ZIFs dosage of 0.3 g.L^{-1}, H_2O_2 concentration of 0.01 mol.L^{-1}, and the initial TC concentration of 30 mg.L^{-1} (Figure 3b). The TC removal efficiency by the CuCo-ZIFs/H_2O_2 system took place relatively quickly, reaching about 86.1% removal efficiency in only 10 min. When increasing the time from 10 to 30 min, TC removal efficiency increased to 93.9%, and then almost levelled out at 40 min and 50 min with a value of 94%. As a result, 30 min was chosen to be a reasonable time to ensure effective TC removal in this study.

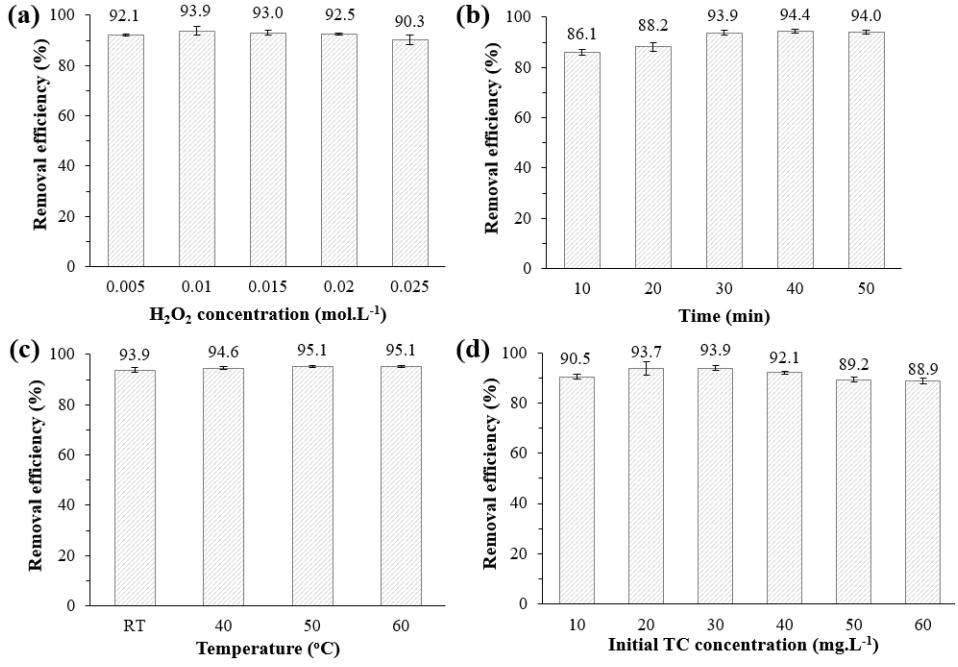

Figure 3. Effect of different parameters on the removal efficiency of TC by CuCo-ZIFs/H_2O_2 system

Except for the investigated parameter, the others were fixed at CuCo-ZIFs dosage = 0.3 g.L^{-1}, H_2O_2 concentration = 0.01 mol.L^{-1}, time = 30 min, room temperature (RT), and initial TC concentration = 30 mg.L^{-1}

Fourthly, the effect of four different temperatures of room temperature, 40ºC, 50ºC, and 60ºC on TC removal efficiency was investigated using CuCo-ZIFs dosage of 0.3 $g.L^{-1}$, H_2O_2 concentration of 0.01 $mol.L^{-1}$, an initial TC concentration of 30 $mg.L^{-1}$ within 30 min (Figure 3c). Theoretically, the higher the temperature, the faster the movement of molecules in the reaction, thereby promoting better TC removal efficiency (Yuan et al., 2020). In fact, when increasing the temperature from room temperature to 40ºC, the removal efficiency of TC increased from 93.9% to 94.6% and tended to balance at 95.1% at temperatures of 50ºC and 60ºC. Accordingly, the TC removal efficiency of the CuCo-ZIFs/H_2O_2 catalyst system was high even at room temperature, which is a good sign for practical applications. Thus, room temperature is suitable for the next experiments.

Finally, the TC removal efficiency was investigated with various initial TC concentrations in the range of 10-60 $mg.L^{-1}$ under the optimal conditions obtained in the above experiments (Figure 3d). As shown in Figure 3d, when the TC concentration increased from 10 $mg.L^{-1}$ to 30 $mg.L^{-1}$, the TC removal efficiency increased proportionally from 90.5% to 93.9%. However, further raises in the TC concentrations, from 30 to 60 $mg.L^{-1}$, resulted in a decrease in the removal efficiency from 93.9% to 88.9%. This can be explained that high TC concentration increases TC density, yet the number of available active sites remains the same because the CuCo-ZIFs dosage is fixed, hence, TC was not effectively removed (Fu et al., 2021). In this study, the initial TC concentration was chosen to be 30 $mg.L^{-1}$.

Besides, CuCo-ZIFs were also compared with some other ZIFs heterogeneous catalysts on the removal of TC (Table 1).

Overall, CuCo-ZIFs showed the highest TC removal efficiency among all the catalysts evaluated in this study. Impressively, the TC removal efficiency of CuCo-ZIFs reached 93.9%, much higher than the monometallic ZIF-8 (Zn-ZIFs) and ZIF-67 (Co-ZIFs) with values of 86.2% and 75.9%, respectively. The outcome indicated that the CuCo-ZIFs/H_2O_2 system carries high potential to remove TC in aqueous solution.

Table 1. Comparison of other heterogeneous catalysts on the removal of TC

Catalyst	The TC removal efficiency (%)	SD
CuCo-ZIFs	93.9	0.9
FeCo-ZIFs	90.0	1.3
FeZn-ZIFs	76.2	1.9
NiZn-ZIFs	80.9	2.9
Co-ZIFs	75.9	2.3
Zn-ZIFs	86.2	2.9

4. CONCLUSION

In conclusion, the bimetallic CuCo-ZIFs were successfully synthesized by combining copper with a monometallic ZIF-67 frameworks *via* a mild ultrasonic-assisted solvothermal method at room temperature. The obtained CuCo-ZIFs had a relatively uniform size with an average particle size of about 150 nm and a high thermal stability of above 500ºC. Beyond that, CuCo-ZIFs demonstrated outstanding catalytic performance in activating H_2O_2 for TC removal due to its diverse composition. The impact of factors on the TC removal was also investigated, and the removal efficiency of TC reached 93.9% under optimal conditions at CuCo-ZIFs dosage of 0.3 $g.L^{-1}$, H_2O_2 concentration of 0.01 $mol.L^{-1}$, initial TC concentration of 30 $mg.L^{-1}$, at room temperature, and within 30 min. Given the outstanding properties and catalytic activity of CuCo-ZIFs in this study, the catalyst demonstrates significant potential for the removal of harmful antibiotic residues from aqueous solutions, offering a promising and effective strategy for practical environmental remediation applications.

ACKNOWLEDGMENT

This research was supported by the B2023-TCT-22 project funding from the Ministry of Education and Training, Viet Nam.

REFERENCES

Abuzalat, O., Tantawy, H., Basuni, M., Alkordi, M. H., & Baraka, A. (2022). Designing bimetallic zeolitic imidazolate frameworks (ZIFs) for aqueous catalysis: Co/Zn-ZIF-8 as a cyclic-durable catalyst for hydrogen peroxide oxidative decomposition of organic dyes in water. *RSC Advances*, *12*(10), 6025-6036. https://doi.org/10.1039/D2RA00218C

Ben, Y., Fu, C., Hu, M., Liu, L., Wong, M. H., & Zheng, C. (2019). Human health risk assessment of antibiotic resistance associated with antibiotic residues in the environment: A review. *Environmental Research*, *169*, 483-493. https://doi.org/10.1016/j.envres.2018.11.040

Dang, H. G., Tuong, V. T., Thu, N. H. T., Van, B. N., Ho, N. T. T., & Pham, V. T. (2021). Bimetallic CuCo-Zeolitic imidazole frameworks (CuCo-ZIFs): Synthesis and characterization. *Can Tho University Journal of Science*, *13*(1), 78-84. https://doi.org/10.22144/ctu.jen.2021.010

Fan, B., Tan, Y., Wang, J., Zhang, B., Peng, Y., Yuan, C.,... Cui, S. (2021). Application of magnetic composites in removal of tetracycline through adsorption and advanced oxidation processes (AOPs): a review. *Processes*, *9*(9), 1644. https://doi.org/10.3390/pr9091644

Fu, H., Wang, R., Xu, Q., Laipan, M., Tang, C., Zhang, W., & Ling, L. (2021). Facile construction of Fe/Pd-doped graphite carbon nitride for effective removal of doxorubicin: Performance, mechanism and degradation pathways. *Applied Catalysis B: Environmental*, *299*, 120686. https://doi.org/10.1016/j.apcatb.2021.120686

Giao, D. H., Yen, P. Q., & Me, P. T. T., Doan Van Hong. (2019). ZIF-67: Synthesis in ethanol and study adsorption capacity on methyl orange. *Can Tho University Journal of Science*, *55*(2), 1-8. https://doi.org/10.22144/ctu.jvn.2019.031

Honarmandrad, Z., Sun, X., Wang, Z., Naushad, M., & Boczkaj, G. (2023). Activated persulfate and peroxymonosulfate based advanced oxidation processes (AOPs) for antibiotics degradation–A review. *Water Resources and Industry*, *29*, 100194. https://doi.org/10.1016/j.wri.2022.100194

Hu, Z., Guo, Z., Zhang, Z., Dou, M., & Wang, F. (2018). Bimetal zeolitic imidazolite framework-derived iron-, cobalt-and nitrogen-codoped carbon nanopolyhedra electrocatalyst for efficient oxygen reduction. *ACS Applied Materials & Interfaces*, *10*(15), 12651-12658. https://doi.org/10.1021/acsami.8b00512

Ighalo, J. O., Rangabhashiyam, S., Adeyanju, C. A., Ogunniyi, S., Adeniyi, A. G., & Igwegbe, C. A. (2022). Zeolitic imidazolate frameworks (ZIFs) for aqueous phase adsorption–a review. *Journal of Industrial Engineering Chemistry*, *105*, 34-48. https://doi.org/10.1016/j.jiec.2021.09.029

Ince, N. H. (2018). Ultrasound-assisted advanced oxidation processes for water decontamination. *Ultrasonics Sonochemistry*, *40*, 97-103. https://doi.org/10.1016/j.ultsonch.2017.04.009

Le, T. T., Dang, B. H., Nguyen, T. Q., Nguyen, D. P., & Dang, G. H. (2023). Highly efficient removal of tetracycline and methyl violet 2B from aqueous solution using the bimetallic FeZn-ZIFs catalyst. *Green Processing and Synthesis*, *12*(1), 20230122. https://doi.org/10.1515/gps-2023-0122

Lei, X., Lei, Y., Zhang, X., & Yang, X. (2021). Treating disinfection byproducts with UV or solar irradiation and in UV advanced oxidation processes: A review. *Journal of Hazardous Materials*, *408*, 124435. https://doi.org/10.1016/j.jhazmat.2020.124435

Lima, V. B., Goulart, L. A., Rocha, R. S., Steter, J. R., & Lanza, M. R. (2020). Degradation of antibiotic ciprofloxacin by different AOP systems using electrochemically generated hydrogen peroxide. *Chemosphere*, *247*, 125807. https://doi.org/10.1016/j.chemosphere.2019.125807

Liu, H., Xu, G., & Li, G. (2021). Preparation of porous biochar based on pharmaceutical sludge activated by NaOH and its application in the adsorption of tetracycline. *Journal of Colloid Interface Science*, *587*, 271-278. https://doi.org/10.1016/j.jcis.2020.12.014

Liu, M. K., Liu, Y. Y., Bao, D. D., Zhu, G., Yang, G. H., Geng, J. F., & Li, H. T. (2017). Effective removal of tetracycline antibiotics from water using hybrid carbon membranes. *Scientific Reports*, *7*(1), 43717. https://doi.org/10.1038/srep43717

Lu, S., Liu, L., Yang, Q., Demissie, H., Jiao, R., An, G., & Wang, D. (2021). Removal characteristics and mechanism of microplastics and tetracycline composite pollutants by coagulation process. *Science of the Total Environment*, *786*, 147508. https://doi.org/10.1016/j.scitotenv.2021.147508

Nidheesh, P., & Rajan, R. (2016). Removal of rhodamine B from a water medium using hydroxyl and sulphate radicals generated by iron loaded activated carbon. *RSC Advances*, *6*(7), 5330-5340. https://doi.org/10.1039/C5RA19987E

Park, K. S., Ni, Z., Côté, A. P., Choi, J. Y., Huang, R., Uribe-Romo, F. J.,... Yaghi, O. M. (2006). Exceptional chemical and thermal stability of zeolitic imidazolate frameworks. *Proceedings of the National Academy of Sciences*, *103*(27), 10186-10191. https://doi.org/10.1073/pnas.0602439103

Takdastan, A., Kakavandi, B., Azizi, M., & Golshan, M. (2018). Efficient activation of peroxymonosulfate by using ferroferric oxide supported on carbon/UV/US system: a new approach into catalytic degradation of bisphenol A. *Chemical Engineering Journal*, *331*, 729-743. https://doi.org/10.1016/j.cej.2017.09.021

Ulu, A. (2020). Metal–organic frameworks (MOFs): a novel support platform for ASNase immobilization. *Journal of Materials Science*, *55*(14), 6130-6144. https://doi.org/10.1007/s10853-020-04452-6

Wang, J.-S. Y., Xiao-Hong, Xu, X., Ji, H., Alanazi, A. M., Wang, C.-C., Zhao, C.,... Yamauchi, Y. (2022). Eliminating tetracycline antibiotics matrix via photoactivated sulfate radical-based advanced oxidation process over the immobilized MIL-88A: Batch and continuous experiments. *Chemical Engineering Journal*, *431*, 133213. https://doi.org/10.1016/j.cej.2021.133213

Wang, H., He, Q., Liang, S., Li, Y., Zhao, X., Mao, L., ... & Chen, L. (2021a). Advances and perspectives of ZIFs-based materials for electrochemical energy storage: Design of synthesis and crystal structure, evolution of mechanisms and electrochemical

performance. *Energy Storage Materials*, *43*, 531-578. https://doi.org/10.1016/j.ensm.2021.09.023

Wang, W., Chen, M., Wang, D., Yan, M., & Liu, Z. (2021b). Different activation methods in sulfate radical-based oxidation for organic pollutants degradation: Catalytic mechanism and toxicity assessment of degradation intermediates. *Science of the Total Environment*, *772*, 145522. https://doi.org/10.1016/j.scitotenv.2021.145522

Wang, Z., Lai, C., Qin, L., Fu, Y., He, J., Huang, D.,... Li, L. (2020). ZIF-8-modified $MnFe_2O_4$ with high crystallinity and superior photo-Fenton catalytic activity by Zn-O-Fe structure for TC degradation. *Chemical Engineering Journal*, *392*, 124851. https://doi.org/10.1016/j.cej.2020.124851

Wang, Z., Lai, C., Qin, L., Fu, Y., He, J., Huang, D., ... & Zhou, X. (2020). ZIF-8-modified MnFe2O4 with high crystallinity and superior photo-Fenton catalytic activity by Zn-O-Fe structure for TC degradation. *Chemical Engineering Journal*, *392*, 124851.

Xu, L., Zhang, H., Xiong, P., Zhu, Q., Liao, C., & Jiang, G. (2021). Occurrence, fate, and risk assessment of typical tetracycline antibiotics in the aquatic environment: A review. *Science of the Total Environment*, *753*, 141975. https://doi.org/10.1016/j.scitotenv.2020.141975

Yang, Z., Jia, S., Zhuo, N., Yang, W., & Wang, Y. (2015). Flocculation of copper (II) and tetracycline from water using a novel pH-and temperature-responsive flocculants. *Chemosphere*, *141*, 112-119. https://doi.org/10.1016/j.chemosphere.2015.06.050

Yao, B., Lua, S.-K., Lim, H.-S., Zhang, Q., Cui, X., White, T. J.,... Dong, Z. (2021). Rapid ultrasound-assisted synthesis of controllable Zn/Co-based zeolitic imidazolate framework nanoparticles for heterogeneous catalysis. *Microporous Mesoporous Materials*, *314*, 110777. https://doi.org/10.1016/j.micromeso.2020.110777

Yao, W., Guo, H., Liu, H., Li, Q., Wu, N., Li, L.,... Yang, W. (2020). Highly electrochemical performance of Ni-ZIF-8/N S-CNTs/CS composite for simultaneous determination of dopamine, uric acid and L-tryptophan. *Microchemical Journal*, *152*, 104357. https://doi.org/10.1016/j.microc.2019.104357

Yuan, M., Fu, X., Yu, J., Xu, Y., Huang, J., Li, Q., & Sun, D. (2020). Green synthesized iron nanoparticles as highly efficient fenton-like catalyst for degradation of dyes. *Chemosphere*, *261*, 127618. https://doi.org/10.1016/j.chemosphere.2020.127618

Zhang, X. W., Lan, M. Y., Wang, F., Wang, C. C., Wang, P., Ge, C., & Liu, W. (2022a). Immobilized NC/Co derived from ZIF-67 as PS-AOP catalyst for effective tetracycline matrix elimination: From batch to continuous process. *Chemical Engineering Journal*, *450*, 138082. https://doi.org/10.1016/j.cej.2022.138082

Zhang, Y., Chu, C., Xu, Y., Ma, Z., & Han, H. (2022b). Bimetallic catalyst derived from copper cobalt carbonate hydroxides mediated ZIF-67 composite for efficient hydrogenation of 4-nitrophenol. *Colloids Surfaces A: Physicochemical Engineering Aspects*, *641*, 128477. https://doi.org/10.1016/j.colsurfa.2022.128477